

ADDITIVE REINFORCED CONCRETE (ARC) FOR MULTIFUNCTIONAL CONSTRUCTION COMPONENT

CHEN XIA¹, CHANG HOON LEE¹, MAX LEIFER², and BUJINGDA ZHENG^{2*}

¹*Dept of Civil and Environmental Engineering, Western New England Univ, Springfield, United States*

²*Dept of Mechanical Engineering, Western New England Univ, Springfield, United States*

Achieving multifunctional structures in construction often requires embedding functional materials into cement-based mortars before additive manufacturing or applying functional layers after solidification. However, these approaches face challenges such as uneven material distribution and mechanical mismatches. Here, the additive reinforced concrete (ARC) manufacturing process, which integrates the end effectors of both fused filament fabrication (FFF) with cement-based mortar extrusion printing (CEP), is presented. This hybrid approach enables the simultaneous deposition of cement-based mortar and fused polymeric filament, with different nozzle configurations allowing the filament to be deposited outside, inside, or sandwiched within the concrete. The ARC manufacturing process facilitates embedding diverse functional components, such as polymers, into freeform 3D printed concrete (i.e., 3D printable cement-based mortars) structures for applications in thermal insulation. Polymeric materials significantly enhance thermal insulation compared to pure mortar, with the performance of polylactic acid (PLA) and polyethylene terephthalate glycol (PETG) evaluated in various configurations within the concrete. This work establishes a scalable pathway for multifunctional concrete structures, advancing innovative and efficient building solutions.

Keywords: Additive manufacturing, Multimaterial, Freeform, 3D printed concrete.

1 INTRODUCTION

The integration of additive manufacturing technology, particularly concrete extrusion 3D printing (CEP), has revolutionized the construction industry by enhancing automation, efficiency, and design flexibility (Khan *et al.* 2024). This approach enables the fabrication of complex and customized structures that traditional methods struggle to achieve. However, despite these advancements, 3D-printed mortar remains functionally limited, lacking the ability to integrate additional materials for enhanced thermal, mechanical, and multifunctional properties. Addressing this limitation requires embedding reinforcements or functional materials into the structures during or after the printing process (Shakor *et al.* 2019).

A widely used approach is pre-mixing functional elements into the mortar before printing. For instance, aerogels have been incorporated to improve thermal insulation (Ma *et al.* 2022), additive mortar (Ma *et al.* 2020) and glass fibers (Shakor *et al.* 2020) have been used to enhance interlayer bonding, and alkali-activated binders with high electrical conductivity enable strain-sensing capabilities in self-sensing cements (Vlachakis *et al.* 2022). However, the pre-mixing method faces

significant limitations: uneven material distribution during mixing, which leads to performance inconsistencies. Additionally, the introduction of functional elements may reduce the printability of the concrete mixture (Jiao *et al.* 2021). On the other hand, the high flowability of concrete mixtures requires vertical material deposition, restricting material integration in freeform structures and limiting overall design flexibility (Wang *et al.* 2023).

Given these challenges, an alternative approach is to introduce functional materials via an independent, controlled deposition process rather than mixing them into the 3D printing mortars. Fused filament fabrication (FFF) has gained attention for its ability to precisely deposit polymeric materials, offering greater control over spatial material placement and the potential for multi-material integration (Zheng *et al.* 2024). This makes FFF a promising candidate for embedding functional components into 3D-printed concrete.

Herein, to overcome the challenges associated with traditional mixing-based strategies, this study introduces the additive reinforced concrete (ARC) manufacturing process, a hybrid multi-material additive manufacturing approach that integrates FFF with CEP. This method provides precise control over the spatial arrangement of cement-based mortar and polymeric materials, enabling the fabrication of multifunctional structures with enhanced thermal, mechanical, and sensing capabilities. The ARC process is implemented through a customized hybrid 3D printing end-effector, allowing the sequential deposition of concrete and commercial polymeric filaments in various configurations. First, FFF fabricates polymeric components using commercially available thermoplastics, such as polylactic acid (PLA) and polyethylene terephthalate glycol (PETG). Next, CEP extrudes the mortar, either casting adjacent to or encapsulating the pre-printed polymer structure. This precisely controlled material placement enables concrete to be strategically deposited around or sandwiched within polymeric elements, serving distinct application purposes such as thermal insulation.

Other than functional integration, ARC also addresses the vertical deposition constraints in concrete 3D printing. Due to the rapid solidification of polymeric materials, FFF-printed elements can act as structural supports for non-vertical concrete deposition, enabling freeform CEP and expanding design flexibility in concrete additive manufacturing.

Overall, the ARC method demonstrates two key advancements: the programmed assembly of functional polymer and concrete and enhanced construction flexibility in additively manufactured concrete. This methodology represents a significant step forward in developing integrated, multifunctional 3D concrete structures, with broad applications in thermal management, embedded sensing, and advanced architectural design.

2 METHOD

2.1 Design of Cement-Based Materials

The mortar material was specifically prepared for 3D printing application. ASTM C150 Type I/II (2023a) cement was utilized, with a water-to-cement ratio of 0.28. Additionally, ASTM C33 (2023b) fine aggregate was incorporated, maintaining a paste-to-aggregate ratio of 0.95. The fine aggregate employed in the experiment has a fineness modulus of 2.31. To prevent potential clogging in the 3D printing auger, the aggregate was further sieved using a No. 50 sieve, corresponding to a nominal sieve size of 300 microns. The materials were mixed in accordance with ASTM C305 (ASTM 2020), with a total mixing time of approximately five minutes.

2.2 Design and Construction of the ARC Platform

The ARC platform was developed by modifying a commercial FFF 3D printer (Neptune 4 Max). A custom cement-based mortar extruder was integrated alongside the FFF hotend to enable multi-



material deposition. The control system was upgraded using an Arduino Mega 2560 R3 microcontroller and a RAMPS 1.6+ control board. The firmware was adapted from the open-source GRBL-MEGA-5X project to support synchronized control of both extrusion systems.

3 RESULTS

As shown in Figure 1(a), the ARC platform operates with three linear degrees of freedom and integrates the FFF hotend with the CEP extruder for efficient tool-switching. When one material is finished printing, the system is programmed to reposition the tool head along the x and y axes by Δx and Δy mm, ensuring that the toolpath for the subsequent material is precisely center-aligned with the previously printed structure (Figure 1(b)).

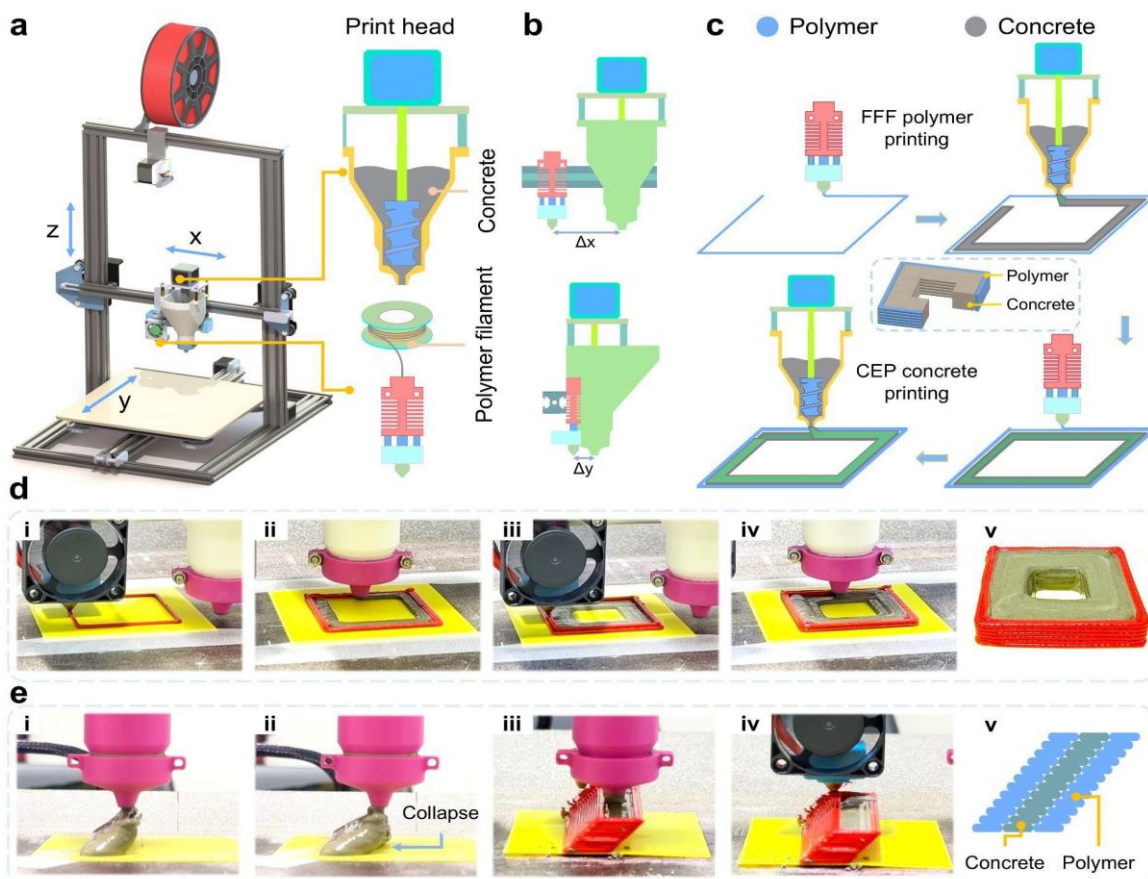


Figure 1. Schematic representation of the ARC platform and its process flow for producing multi-material structures by integrating polymeric and cement-based mortar components: (a) schematic of the ARC platform and its integrated 3D printing end-effectors; (b) relative installation offsets between the FFF hotend and the CEP extruder; (c) process workflow for manufacturing a sample integrating cement-based mortar and polymer by ARC; (d) time-lapse sequence of fabrication steps for a concrete-polymer sample; (e) comparison between cement printing with and without polymer support.

To illustrate the ARC process, a PLA-concrete bi-material sample was fabricated (Figures 1(c) and (d)). The fabrication process began with the FFF deposition of a single layer of PLA, forming a square frame (Figure 1(d-i)). The PLA filament was printed at 220 °C with a layer height of 1

mm to provide a stable boundary for the subsequent concrete deposition. Following this, the system switched to the CEP extruder, which deposited a concrete layer within the PLA frame (Figure 1(d-ii)). The concrete mixture was extruded at the center of the PLA frame using a 4 mm nozzle, with a layer height of 1 mm to ensure uniform z-axis alignment.

The ARC process continued by alternating deposition between the FFF and CEP systems, sequentially printing a second PLA frame layer followed by an additional mortar layer (Figure 1(d-iii) and (d-iv)). This layering strategy facilitated consistent material integration across all layers, ensuring a structurally cohesive interface.

The completed sample is shown in Figure 1(d-v). Visual inspection of the fabricated structure confirmed accurate alignment between the PLA and mortar components, with no visible delamination or displacement at the material interface. Additionally, the FFF-printed PLA frame acted as a structural guide during concrete placement, preventing early-stage deformation and maintaining spatial precision.

Additionally, the freeform CEP is demonstrated in Figure 1(e). Figures 1(e-i) and (e-ii) illustrate that the inclined mortar sample collapses without a supporting structure due to its flowability. In contrast, Figures 1(e-ii) and (e-iv) demonstrate that, with the polymer material as support, the inclined mortar sample can be successfully constructed. The schematic of the supporting structure is shown in Figure 1(e-v).

To analyze how polymeric materials used as insulation layers influence building energy consumption, both bare concrete with mortar (10%) and concrete with two types of insulation (PLA and PETG) were applied to an IECC (International Energy Conservation Code) residential prototype Detached (single-family) House model and the energy consumption patterns were simulated through DesignBuilder, a state-of-the-art software tool for checking building energy, carbon, lighting, and comfort performance (Figure 2). The Model is a typical two-story, three-bedroom, slab-on-grade detached house with no garage and is assumed to be located in Boston climate zone 5A.

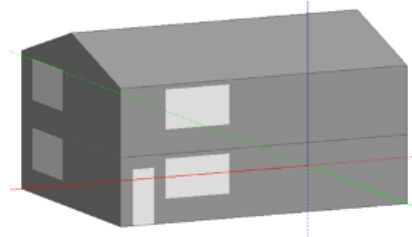


Figure 2. IECC residential prototype detached house model (two-story, three-bedroom, slab-on-grade, no garage) used in DesignBuilder simulations to evaluate the effect of PLA and PETG insulation layers on building energy consumption in Boston climate zone 5A.

Table 1 shows the simulation results comparing the thermal performance and associated energy consumption of the model as increasing PLA and PETG insulation layers at various densities. It is evident that incorporating PLA and PETG significantly improved the insulation properties, as demonstrated by their higher R-values and correspondingly lower U-values compared to the mortar with no insulation. Specifically, the PLA insulation shows better thermal performance, leading to lower energy consumption for both heating and cooling, especially noticeable in the higher-density variations (e.g., PLA 0.0012) which showed a substantial reduction in heating demand (13,242.85 kWh) compared to concrete alone (17,390.10 kWh). PETG insulation also improved performance with a lesser extent than PLA, with intermediate results for heating and cooling energy usage.

These findings align with research by Xia and Hu (2024), which emphasizes the significant impact of building characteristics on residential energy consumption patterns.

Table 1. Thermal properties and annual energy consumption.

		Thickness (mm)	R value (m ² K/W)	U value (W/m ² K)	Heating (kWh)	Cooling (kWh)
1	Reference (mortar)	250	0.175	5.714	17390.10	11875.92
2	PLA 0.0004	250	0.254	3.937	14031.96	12503.28
3	PLA 0.0008	250	0.257	3.891	13927.84	12525.26
4	PLA 0.0012	250	0.264	3.788	13242.85	11825.49
5	PETG 0.0004	250	0.215	4.651	15010.92	11440.06
6	PETG 0.0008	250	0.221	4.524	15274.32	12250.40
7	PETG 0.0012	250	0.222	4.505	15233.68	12258.15

Detailed consumption patterns of bare concrete and PLA 0.0012 were also compared. The simulation results (Figure 3) indicate the differences in energy consumption patterns throughout the year. Specifically, the bare concrete scenario (Figure 3, top) displays significantly higher peaks in heating demand during colder months, particularly January, February, November, and December, indicating poor thermal insulation performance. In contrast, the scenario with PLA 0.0012 insulation (Figure 3, bottom) shows substantially reduced heating demands in the same periods, illustrating improved heat retention. Additionally, cooling loads during warmer months appear slightly lower for PLA 0.0012 insulation compared to bare concrete, signifying a more balanced thermal environment and reduced reliance on mechanical cooling systems. These results demonstrate that embedding PLA insulation considerably mitigates seasonal peaks in heating and cooling demands, resulting in improved overall energy efficiency and thermal comfort for residential buildings in climate zones comparable to Boston.

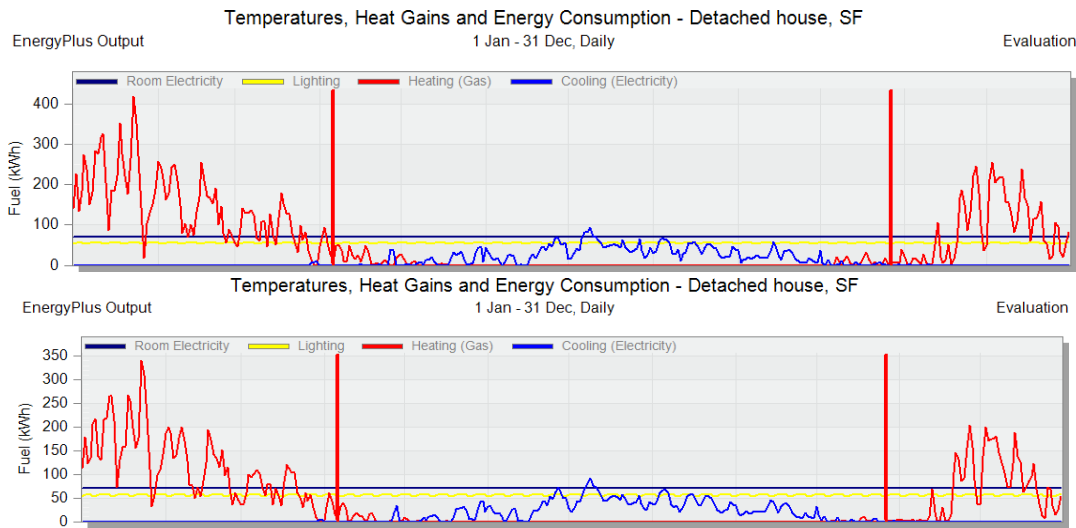


Figure 3. Annual energy consumption patterns: bare concrete (top) vs. PLA 0.0012 (bottom).

4 DISCUSSIONS AND CONCLUSIONS

The ARC process enables the integrated fabrication and spatial assembly of polymeric and cement-based mortar within a unified multi-material printing workflow. The polymeric components

include PLA, PETG, conductive thermoplastics, and other materials compatible with FFF. As a proof of concept, two functional applications were demonstrated: a thermally insulating the mortar block and a cement-based mortar with embedded capacitive sensor. In addition to serving as functional elements, polymeric materials can also act as support structures, thereby enabling freeform cement-based mortar printing. This addresses the long-standing vertical deposition constraint inherent to conventional CEP. No delamination was observed at the cement-polymer interface (Figure 1(d)), suggesting adequate interlock from the layered deposition and thermal conditions. Prior work (e.g., Zheng *et al.* 2024) supports the role of polymer geometry in enhancing structural stability. Bond strength testing is planned for future work. Currently, the ARC process has been validated on a desktop-scale system. To unlock its full potential for large-scale construction applications, the system must be scaled up to industrial-grade hardware. Ultimately, ARC provides a scalable and versatile approach for constructing multifunctional concrete elements with embedded performance-enhancing features, advancing the development of intelligent and adaptable infrastructure systems.

References

- ASTM, *ASTM C150/C150M-23: Standard Specification for Portland Cement*, ASTM International, West Conshohocken, PA, 2023a.
- ASTM, *ASTM C33/C33M-23: Standard Specification for Concrete Aggregates*, ASTM International, West Conshohocken, PA, 2023b.
- ASTM, *ASTM C305-20: Standard Practice for Mechanical Mixing of Hydraulic Cement Pastes and Mortars of Plastic Consistency*, ASTM International, West Conshohocken, PA, 2020.
- Jiao, D., De Schryver, R., Shi, C., and De Schutter, G., *Thixotropic Structural Build-Up of Cement-Based Materials: A State-of-The-Art Review*, Cement and Concrete Composites, Elsevier, 122, 104152, September 2021.
- Khan, S. A., Ghazi, S. M. U., Amjad, H., Imran, M., and Khushnood, R. A., *Emerging Horizons in 3D Printed Cement-Based Materials with Nanomaterial Integration: A Review*, Construction and Building Materials, Elsevier, 411, 134815, January 2024.
- Ma, G., Ruhan, A., Xie, P., Pan, Z., Wang, L., and Hower, J. C., *3D-Printable Aerogel-Incorporated Concrete: Anisotropy Influence on Physical, Mechanical, and Thermal Insulation Properties*, Construction and Building Materials, Elsevier, 323, 126551, March 2022.
- Ma, G., Salman, N. M., Wang, L., and Wang, F., *A Novel Additive Mortar Leveraging Internal Curing for Enhancing Interlayer Bonding of Cementitious Composite for 3D Printing*, Construction and Building Materials, Elsevier, 244, 118305, May 2020.
- Shakor, P., Nejadi, S., Paul, G., and Malek, S., *Review of Emerging Additive Manufacturing Technologies in 3D Printing of Cementitious Materials in the Construction Industry*, Frontiers in Built Environment, Frontiers, 4, 85, January 2019.
- Shakor, P., Nejadi, S., Sutjipto, S., Paul, G., and Gowripalan, N., *Effects of Deposition Velocity in the Presence/Absence of E6-Glass Fibre on Extrusion-Based 3D Printed Mortar*, Additive Manufacturing, Elsevier, 32, 101069, March 2020.
- Vlachakis, C., McAlorum, J., and Perry, M., *3D Printed Cement-Based Repairs and Strain Sensors*, Automation in Construction, Elsevier, 137, 104202, May 2022.
- Wang, L., Ye, K., Wan, Q., Li, Z., and Ma, G., *Inclined 3D Concrete Printing: Build-Up Prediction and Early-Age Performance Optimization*, Additive Manufacturing, Elsevier, 71, 103595, June 2023.
- Xia, C., and Hu, Y., *Profiling Residential Energy Vulnerability: Bayesian-Based Spatial Mapping of Occupancy and Building Characteristics*, Sustainable Cities and Society, Elsevier, 114, 105667, November 2024.
- Zheng, B., Xie, Y., Xu, S., Meng, A. C., Wang, S., Wu, Y., Yang, S., Wan, C., Huang, G., Tour, J. M., and Lin, J., *Programmed Multimaterial Assembly by Synergized 3D Printing and Freeform Laser Induction*, Nature Communications, Springer Nature, 15, 4541, May 2024.

